Diagn Interv Radiol 2022; 28:50–57

HEAD AND NECK IMAGING

ORIGINAL ARTICLE

X-linked deafness/incomplete partition type 3: Radiological evaluation of temporal bone and intracranial findings

Safak Parlak
Ekim Gumeler
Levent Sennaroglu
Burce Ozgen

PURPOSE
X-linked deafness (XLD) is a rare disease characterized by typical cochlear incomplete partition type 3 (IP-III) anomaly. Accompanying hypothalamic anomalies were also recently described. The purpose of this study was to document the temporal bone and intracranial imaging findings in a series of patients with XLD, with a review of the literature, to better understand this anomaly.

METHODS
The computed tomography and magnetic resonance imaging studies of 13 XLD patients were retrospectively evaluated. All structures of the otic capsule (OC) were subjectively and retrospectively assessed. The OC thickness and the size of the cochlea were measured and compared to the age-matched control group. Intracranial structures were also evaluated with specific attention to the hypothalamic region.

RESULTS
All cases had bilateral IP-III anomaly, bulbous internal auditory canals (IACs), absent bony modiolus with preserved interscalar septa, and intact cochleovestibular and facial nerves. The thickness of the OC was decreased in all cases compared to the control group ($P < .001$). In XLD patients, the cochlea had decreased in the transverse dimension and increased in height compared to the control group ($P < .001$). Five patients (38.4%) had bilateral cystic structures adjacent to the vestibule and/or semicircular canals (SCCs). The hypothalamus was thickened or had a lobular appearance in all cases (subtle in one). Additionally, hamartoma-like appearance of the hypothalamus was present in half of the cases.

CONCLUSION
XLD is a rare inner ear anomaly that is frequently associated with hypothalamic malformations. The OC thickness of IP-III patients appears to be decreased with accompanying decreased transverse dimension of the cochlea, which could have implications in electrode selection during cochlear implantation. Cystic/diverticular lesions surrounding the vestibule and semicircular canals are also frequently seen but rarely reported findings.

X-linked deafness (XLD), also known as DFNX2, is one form of X-linked non-syndromic hearing loss. This is a rare genetic disease caused by mutation in the *POU3F4* gene, characterized by bilateral mixed hearing loss and high risk of perilymph gusher at stapes surgery. XLD is characterized by symmetrical cochlear incomplete partition type 3 anomaly (IP-III). IP-III has pathognomonic imaging findings including the absence of spiral lamina, bony modiolus, and cribriform plate that separates the base of the cochlea and the internal auditory canal (IAC) as well as the presence of a dilated IAC.[1,2] Enlarged tympanic and labyrinthine segments of the facial nerve canal, malformed vestibules, semicircular canals (SCCs), and enlarged vestibular aqueduct has also been reported.[1,3,4] Patients with XLD have been reported to have preserved a cochlear size and intact cochleovestibular nerves.[5,6] Abnormal diverticular cystic bulge of the vestibule and SCCs have also been reported with XLD.[3,6] Additionally, malformations in the hypothalamus were also recently reported in patients with this anomaly.[3,7-10]

From the Departments of Radiology (S.P. ✉ *parlaksafak@gmail.com*, E.G.) and Otorhinolaryngology (L.S.), Hacettepe University Faculty of Medicine, Ankara, Turkey; Department of Radiology (B.O.M.), University of Illinois at Chicago, Chicago, Illinois, USA.

Received 2 October 2020; revision requested 28 October 2020; last revision received 20 January 2021; accepted 31 January 2021.

Published online 16 August 2021.

DOI 10.5152/DIR.2021.20791

You may cite this article as: Parlak S, Gumeler E, Sennaroglu L, Ozgen B. X-linked deafness/incomplete partition type 3: Radiological evaluation of temporal bone and intracranial findings. *Diagn Interv Radiol*. 2022;28(1):50-57.

In this study, we aimed to examine temporal bone findings as well as the accompanying intracranial findings in a series of patients with XLD, to further evaluate the characteristics of the disease that might impact the care of patients.

Methods

Patients

A database search was performed to identify all patients with imaging diagnosis of IP-III anomaly, scanned between January 2005 and January 2019. Inclusion criteria were patients with typical computed tomography (CT) findings who had their baseline temporal bone imaging available in the PACS database (n=13). Additionally, 13 age-matched temporal bone CTs with normal inner ear findings, performed for causes other than congenital hearing loss, were also selected as the control group, for comparative evaluation. The study was approved by our Institutional Review Board and informed consent was waived due to the retrospective design of the study (GO2020/02-06).

Image acquisition

CT images of the temporal bones were obtained in the axial plane using a multidetector scanner (Somatom Plus 4/Volume Zoom, Siemens), with 0.5 mm collimation and 0.5 mm slice thickness. The data set acquired for each patient was used to create axial and coronal reformatted images, parallel and perpendicular to the lateral SCCs, respectively. Magnetic resonance imaging (MRI) examinations were performed with either a 3T (Ingenia, Philips or Allegra, Siemens) or a 1.5T scanner (Symphony, Siemens), by using a standard head coil. All scans included axial and sagittal oblique three-dimensional (3D) constructive interference in steady-state (CISS) or driven equilibrium radiofrequency reset pulse (DRIVE).

Imaging evaluation

CT and MRI examinations were subjectively and retrospectively evaluated by a neuroradiologist experienced in head and neck imaging. The structures evaluated with qualitative assessment included stapes and oval window, cochlear appearance, interscalar septa (ISS), modiolus, spiral lamina, vestibule, superior and inferior vestibular canals, SCCs, vestibular aqueduct, facial canal, IAC. The presence of cystic structures, defined as abnormal diverticular cystic bulges continuous or adjacent to the vestibule or SCCs, were also noted. The cochleovestibular nerve appearance and size were also assessed on sagittal-oblique high T2-weighted images. Additionally, the available MRI studies were also evaluated with respect to possible anomalies or variations involving the posterior fossa structures and hypothalamus.

The thickness of the otic capsule (OC) and the size of the cochlea were quantitatively measured. The OC thickness was measured anterior to the cochlea, from the anterior aspect of the cochlear apex to the anterior cortical margin (Figure 1). Cochlear size (height and transverse dimension) was also measured in the axial plane in both XLD patients and the control group (Figure 1). As the cochlea in IP-III has a funnel-shaped dysmorphism where the transverse cochlear dimension appears to be narrowed at the level of the middle turn, the transverse dimension was measured from the level of the middle turn. Coronal cochlear height (CCH) was also measured on a coronal section from the midpoint of the basal turn to the midpoint of the apical turn and used for definition of cochlear hypoplasia (defined as CCH <4.25 for females and <4.48 for males based on the work of Mori et al.).[11] All measurements of XLD patients were correlated with measurements of cases in the age-matched control group.

Clinical evaluation

Operative reports of cases who had undergone surgery were also retrospectively reviewed and were classified in terms of cerebrospinal fluid complications. The patients' charts were assessed with respect to the presence of neurological signs/symptoms and for possible endocrine malfunction.

Statistical analysis

Mean, standard deviation (SD), and median (min/max) values were given for variables with normal distribution and without normal distribution, respectively. The normality assumption was assessed by the Kolmogorov–Smirnov test. Categorical variables were given as percentages. To compare controls and patients, the two-sample t test was used for variables with normal distribution, and the Mann–Whitney U test was used for non-normally distributed variables. The result was considered statistically significant when $P < .05$. All analyses were performed using IBM SPSS Statistics 23.0.

Results

The study group consisted of 13 XLD patients. The median age was 4 years (min, 7 months; max, 53 years). Ten of the patients

Main points

- In IP-III anomaly, decreased transverse and slightly increased vertical dimensions of the cochlea are frequent but rarely reported findings, which could affect the selection of the cochlear implant type.
- Decreased otic capsule thickness and cystic/diverticular lesions contiguous with inner ear structures in IP-III are accompanying features that are less frequently mentioned in the literature.
- Malformations in the hypothalamus are frequently found associated with IP-III incomplete partition type 3, with unknown clinical significance.

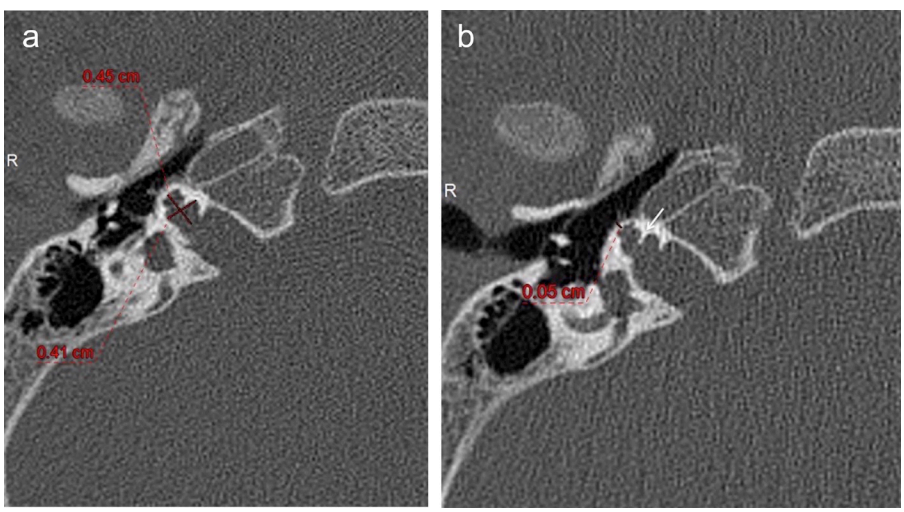

Figure 1. a, b. Measurements of cochlear height and transverse diameter (**a**) with the measurement of the OC thickness (**b**) on an XLD patient. There is also thinning of the OC (**a, b**) and thick ISS (*arrow*).

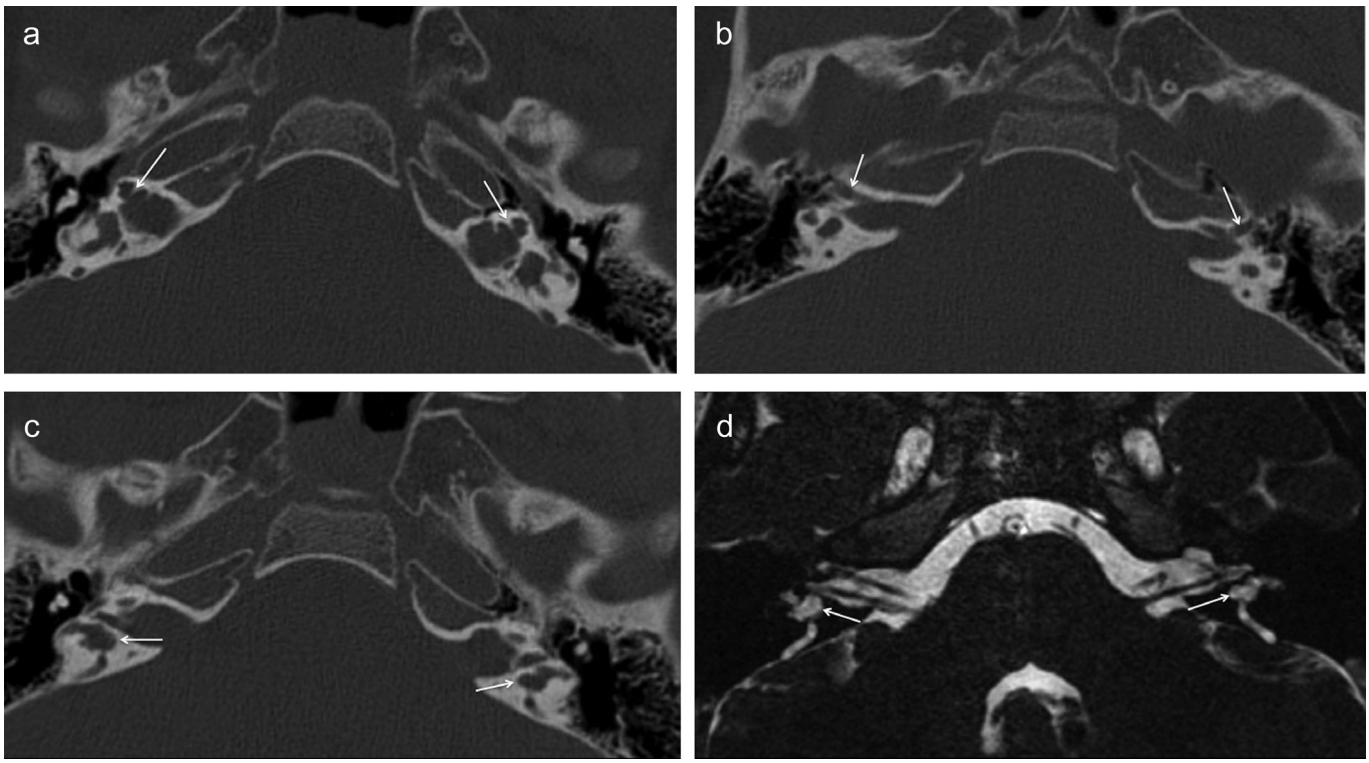

Figure 2. a-d. CT (**a-c**) and MR (**d**) images of a 3-year-old male XLD patient with IP-III anomaly. The images demonstrate bilateral bulbous IACs, absence of cribriform plate and modiolus, and a corkscrew-shaped cochlea with thickening of the ISS (**a**, *arrows*). Notice the subtle widening of the labyrinthine segments of facial canals bilaterally (**b**). Small cystic structures/diverticula (*arrows*) are seen adjacent to the vestibules (**c**, **d**).

were younger than 18. All patients but one were male (M : F, 12 : 1). Several patients belonged to a single family (Patient 6 and Patient 7 were siblings; similarly Patients 8, 9, and 10 were also siblings. Additionally, Patient 7 was the grandfather of Patients 8, 9, and 10).

None of the patients had an endocrinological disorder or seizures. All patients presented with mixed type hearing loss. Seven patients had a history of gusher during cochlear implantation, and the remaining patients had not undergone surgery.

All cases had bilateral typical IP-III anomaly with absent lamina cribrosa and modiolus (Figure 2). The basal turn of the cochlea was widened bilaterally in 5 patients, and the turns of the cochlea were preserved in all subjects. Interscalar septa were preserved in all cases but were thickened peripherally in 12 patients (92.3%) (Figures 2 and 3). All cases had large IACs. Eight patients (61.5%) had dilated inferior vestibular nerve canals (bilaterally in 4 patients and unilaterally in 4 patients). Ten patients (76.9%) had dilated superior vestibular nerve canals. The facial nerve canal was enlarged bilaterally in all patients except one (92.3%) (Figure 2). The labyrinthine segment was the most commonly affected part (92.3%), with the tympanic segment widened in half of the cases. One patient (7.6%) had a bilateral aberrant facial nerve canal. Seven patients had cystic dilatation of vestibular aqueducts bilaterally and one patient had dilated vestibular aqueduct unilaterally on CT (57.6% in ears with XLD). All patients had bilaterally enlarged vestibules. Five patients had cystic/diverticular lesions continuous with the vestibule (38.4%) bilaterally, which were mild in 3 and extensive in 2 patients (Figures 2, 4, and 5).

All cases except 2 (84.6%) revealed dilated SCCs with accompanying bilateral multiple abnormal cystic/diverticular lesions continuous with the dilated SCCs in 2 cases (15.3%) (Figures 4 and 5).

The incidence of semicircular canal dehiscence (SCCD) was 46.1% (n=6). All SCCDs but one were located in the posterior SCC.

Stapes footplates were observed to be thick in 10 patients (bilaterally in 9 of 10 patients) with a rate of 73% in all ears with IP-III. Oval window atresia was observed in 5 patients (which was bilateral in 4 patients, 34.6% in ears with IP-III), and the oval window was severely hypoplastic in the other 4 patients bilaterally (30.7% in ears with IP-III). One of the patients had unilateral stapedial dislocation (3.8%).

OC thickness was decreased in all IP-III cases (median, 0.5 mm; min-max, 0.3-0.7 mm) compared to the OC thickness of the control group (median, 1.1 mm; min-max, 0.8-1.9 mm) and the difference was statistically significant ($P < .001$, Mann–Whitney U test) (Table).

Cochlear mid-turn transverse diameter was significantly lower in XLD patients (mean±SD, 3.99±0.488 mm) than in the control group (5.18±0.454 mm) ($P < .001$, independent samples t test) (Table). Cochlear height was significantly higher in XLD patients (3.73±0.462 mm) than in the control group (3.09±0.411 mm) ($P < .001$, independent samples t test) (Table). Mean cochlear height on coronal images (4.18±0.274 mm) was significantly lower than in the age-matched control group (5.16±0.340 mm) ($P < .001$, independent samples t test) (Table). Eleven patients (84.6%) had hypoplastic CCH.

Ten patients had MRI examinations (6 cases on 1.5T and 4 on 3T scanners). All cases had bilateral typical IP-III anomaly with large IACs. The modiolus and lamina spiralis were absent. Scala vestibuli and

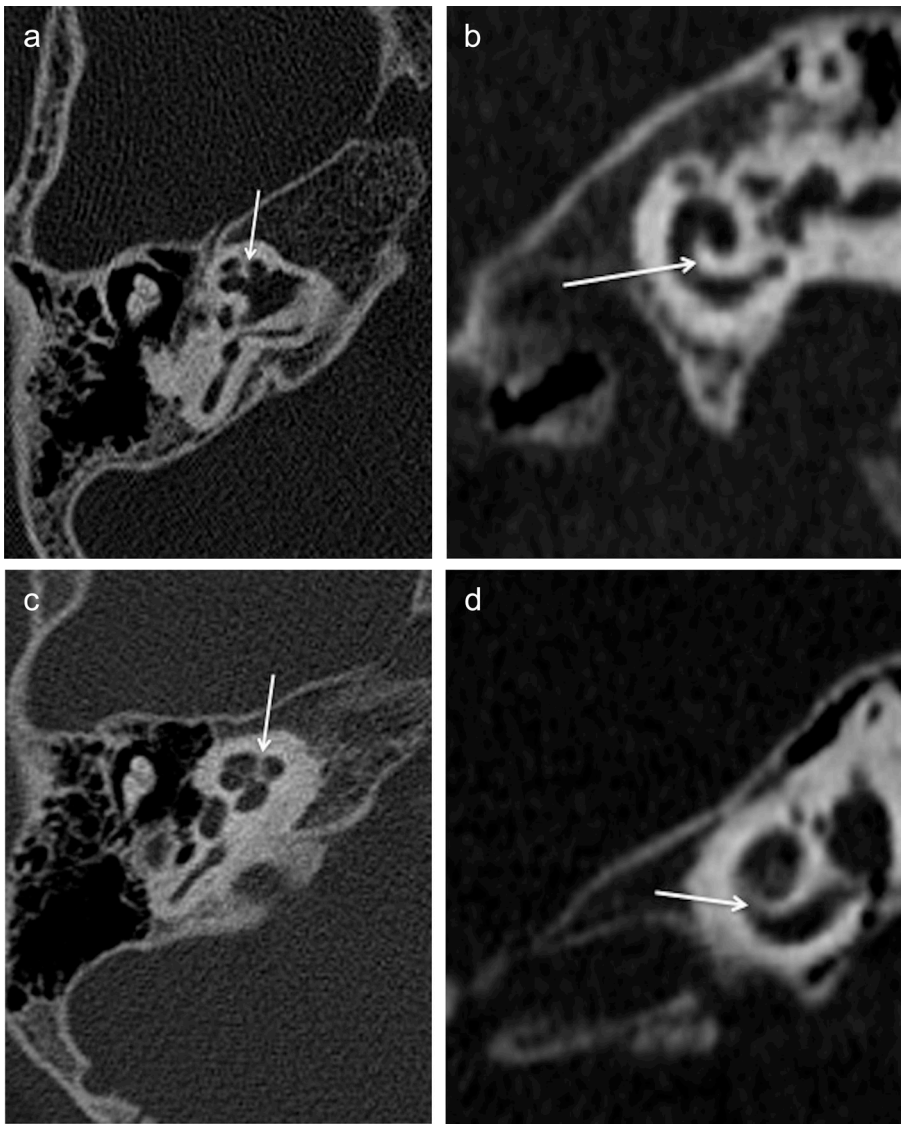

Figure 3. a-d. CT imaging findings of a 2-year-old male patient with XLD. Absent cribriform plate and modiolus of the cochlea with thickened interscalar septa (**a, b,** *arrows*). CT images of a 2-year-old patient with normal inner ear findings for comparison (**c, d**).

scala tympani could not be seen as separate chambers (Figure 6).

All patients had bilaterally intact cochleovestibular and facial nerves. The appearance of cochlear-vestibular and facial nerves on sagittal-oblique images in IAC showed atypical appearance, with curved/comma-shaped appearance of the cochlear nerve (Figure 7). Two patients had unilateral hypoplastic cochlear nerves (defined as a cochlear nerve diameter smaller than the facial nerve diameter on sagittal-oblique high T2-weighted images). Seven patients had normal cochlear nerves. Cochlear nerves of one patient could not be sufficiently evaluated because of inadequate resolution on sagittal-oblique high T2-weighted images. The rate of cochlear nerve hypoplasia was 11.1% in ears with XLD, in patients with adequate sagittal-oblique high T2-weighted images available.

There were no brain stem, posterior fossa, or skull base anomalies, and the pituitary gland was normal in all cases.

Typical dysmorphic features of the hypothalamus were seen in all cases as subtly thickened (n=2; 20%) to a hamartoma-like appearance (n=5; 50%) (Figure 8).

All patients had hypothalamic malformations (marked in 9 patients and subtle in one) that were asymmetric in 5 patients, and with a wrinkly appearance in 6 patients, and a bulky appearance in 3 patients (Figure 8).

Discussion

XLD, first described in 1971, is one of the rare forms of inner ear malformation and constitutes 2% of inner ear malformations.[12,13] Due to the gusher phenomenon, it is also named as X-linked stapes gusher syndrome. Patients usually present with sensorineural hearing loss or mixed type hearing loss with an accompanying conductive component due to stapedial fixation. Females with this mutation usually show no evidence of hearing loss.[14]

The typical inner ear findings of XLD are bilateral IP-III anomaly with bulbous IAC, absent bony modiolus and cribriform plate, and preserved but thickened ISS. Wide facial nerve canal and malformed vestibule and SCCs have also been reported. For the pathophysiology of IP-III, Sennaraoglu et al.[15] suggested that

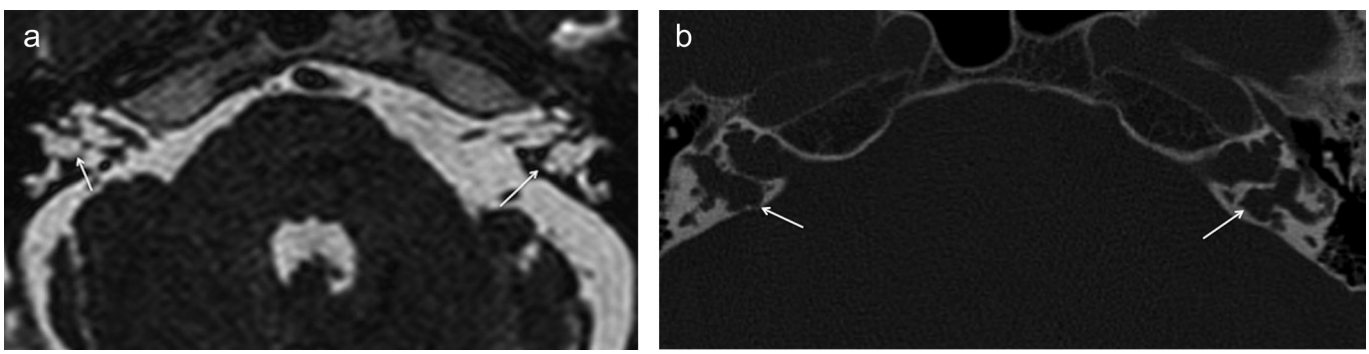

Figure 4. a, b. A 53-year-old male patient with XLD and bilateral typical IP-III. The CT (**a**) and MR (**b**) images demonstrate fluid-filled cavities/cystic structures (*arrows*) surrounding the vestibules and SCCs.

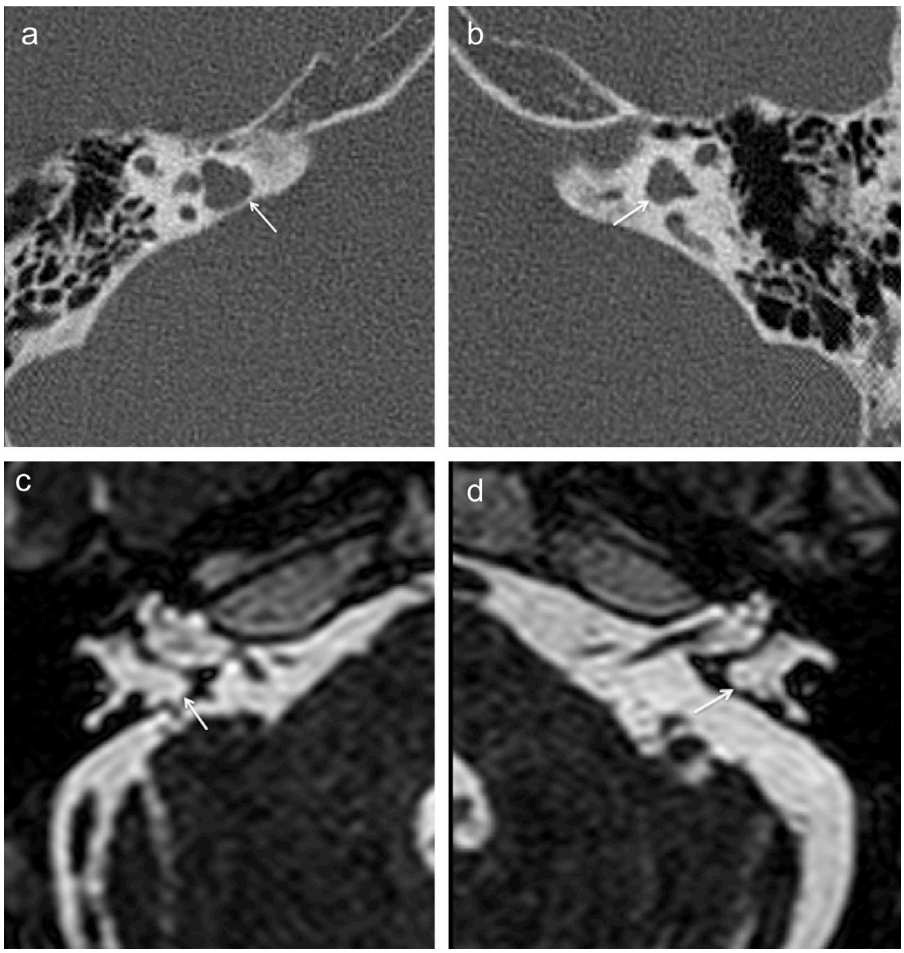

Figure 5. a-d. Bilateral cystic structures in the subarcuate fossa. CT image of a 47-year-old male patient with XLD (**a, b**). MR image (**c, d**) of a 53-year-old male patient with XLD in the same family as the patient in (**a, b**).

Table. Comparison of patients with XLD and controls

Variables	Ears with XLD (n=26)	Controls (n=26)	*P*
Age (years)	4 (7 months, 12-53 years)	7 (8 months, 12-56 years)	.198
Otic capsule thickness (mm)	0.5 (0.3-0.7)	1.1 (0.8-1.9)	<.001
Cochlear transverse diameter (mm)	3.99 ± 0.488	5.18 ± 0.454	<.001
Cochlear height (mm)	3.73 ± 0.462	3.09 ± 0.411	<.001
Coronal cochlear height (mm)	4.18 ± 0.274	5.16 ± 0.340	<.001

Values are expressed as median (min-max) or mean ± SD.

the anomaly might be due to genetic alterations that resulted in abnormal fetal vascular supply from middle ear mucosa. This anomalous vascular supply might prompt defective development of the endochondral and periosteal layers of the OC. Hence, the OC has only an endosteal layer which results in a defect at the cochlear base and modiolus.[15] In accordance with this theory, the thickness of the OC was decreased in all patients. It is known that the *POU3F4* gene has a prominent role in early development in the OC and maturation of bony labyrinth and that it is expressed in the otic mesenchymal cells. POU3F4 deficiency was found to cause defects in both otic fibrocytes and stria vascularis.[16] However, it is unclear how those affected fibrocytes might act in the OC developmental processes (especially if they play a role in vascular development of the OC), or whether there are other vascular effects of POU3F4 deficiency that might result in the suggested vascular compromise theory.

Symmetrical inner ear anomalies such as bulbous IAC, incomplete separation of the cochlea from the IAC, wide facial canal, and absent modiolus were reported as main features on CT.[1,2] In our series, all cases had bilateral typical IP-III anomaly with the absence of cribriform plate, lamina spiralis, and modiolus. The IACs were bulbous in all, with widened facial canals in the majority of cases. The endosteal layer, with the lack of endochondral and outer periosteal layers, may be insufficient to provide compact tissue and may be the reason for bulbous enlargement of the IAC, just like the widening of the tympanic and labyrinthine segments of the facial nerve canal. We noticed a curved/comma-shaped appearance extending infero-posteriorly from the cochlear nerve. A similar appearance was also recently reported by Hong et al.,[17] who described it as a "hypointense spiral structure" and explained it as the membranous labyrinth extending into the dilated IAC due to the incomplete separation of the cochlear base from the IAC. However, the appearance is more likely to represent elongated and stretched inferior vestibular–cochlear anastomoses.[18] The implications of this appearance are unknown at this point.

The lack of incomplete separation of the cochlea from the IAC (due to absent cribriform plate and modiolus) is known to cause incorrect placement of the cochlear implant electrode, which might be displaced into the IAC in 11%-20% of cases.[19, 20] Similarly, in one of our implanted cases, the electrode array had to be repositioned during surgery due to IAC displacement initially.

In most of the cases reported in the literature, the cochlear size was noted to be normal in IP-III anomalies. In a recent paper by Hong et al.,[17] the dimensions of the cochlea were reported to be slightly smaller than normal. In our study, the cochlea was noted to have a dysmorphic appearance with decreased transverse dimension on axial images, decreased coronal height, but increased vertical dimension on axial images compared to the control group. Smeds et al.[19] have previously reported that the full-length insertion of the electrode array could not be performed in 4 cases. Additionally, Alballaa et al.[20] reported that they had obtained full insertions in their cases with a shorter array. Accordingly, in

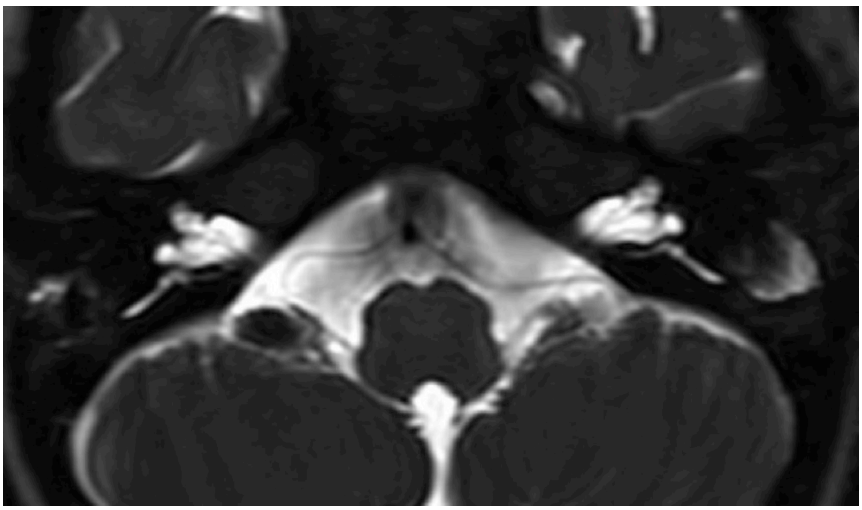

Figure 6. Dysmorphic appearance of the cochlea of a 5-year-old XLD patient. Modiolus cannot be seen.

our series, mid-sized electrodes were used with full insertion in all cases. This subtle decrease in cochlear size in IP-III might thus have implications in the setting of electrode selection for cochlear implantation.

ISS thickening, which can be observed on CT in XLD, has been previously described.[15] In our series, all patients had preserved ISS compatible with literature, but all except one had ISS thickening as well (92.3%). Additionally, 76.9% of the patients had stapes footplate thickening. ISS, as well as the vestibular surface of the stapes, develop from the endosteum.[15] We speculate that in XLD, in the setting of absent/hypoplastic endochondral and outer periosteal layers, the endosteum might have areas of focal hyperplasia, resulting in thickened ISS and stapes footplate.

Malformed vestibules with small outpouchings and irregular SCCs in XLD have also been reported.[21] Anderson et al.[3] reported diverticular outpouchings of vestibules and SCCs in 2 brothers with a diagnosis of XLD. In our study, cystic cavity-like structures were also seen adjacent to the vestibule in up to 38.4% of cases. Additionally, cystic appearances were also noted surrounding the bilateral SCCs. The cystic lesions were also seen at younger ages (in 3 and 5-year-old patients and as early as the first 7 months of life). These neonatal and pediatric cases suggest that these cystic formations are probably developmental in nature. During the embryologic development of the inner ear structures, the ossification of the OC is preceded by a process of cartilage resorption and replacement by vascular connective tissue.[22] The resorption process is due to cell necrosis and liquefaction of the cartilage matrix, followed by blood vessels entering the cartilage and replacing it with vascular connective tissue, which will be ossified later.[22] This process uniformly begins at the subarcuate fossa but the necrotic process seems to be especially prominent in the regions of the posterior and superior canals.[22] Normally, the vascular connective tissue channels are gradually replaced by bone and bone marrow during the ossification stage. The location of the above-mentioned cystic structures in XLD patients raises the possibility that these appearances might be due to a defective ossification of the embryonic vascular connective tissue replacing the liquefied cartilage matrix, or the incomplete/inadequate replacement of these liquefied areas by the vascular connective tissue. It is, of course, unclear what the content of those cystic areas is and whether they contain perilymph, given the fact that they appear to be contiguous with the inner ear structures and especially the SCCs.

SCCD in XLD has been previously reported in the literature and it was present in up to 46.1% of our cases, more frequently seen than previously reported.[23] This finding may be the result of the above-described deficient ossification or underdevelopment of bone overlying the SCCs. If this entity is indeed more frequent than reported, as in our series, it might result in the third-window effect and may be partly responsible for the conductive component of the hearing loss, in addition to the stapedial fixation.

Hypothalamic hamartomas are mostly sporadic and have often been linked to somatic mutations in the *GLI3* gene. Several cases have also been reported with hypothalamic hamartomas with some syndromes including oral-facial-digital syndrome.[24-31] First, Whitehead et al.[9] reported hypothalamic malformation with tuber

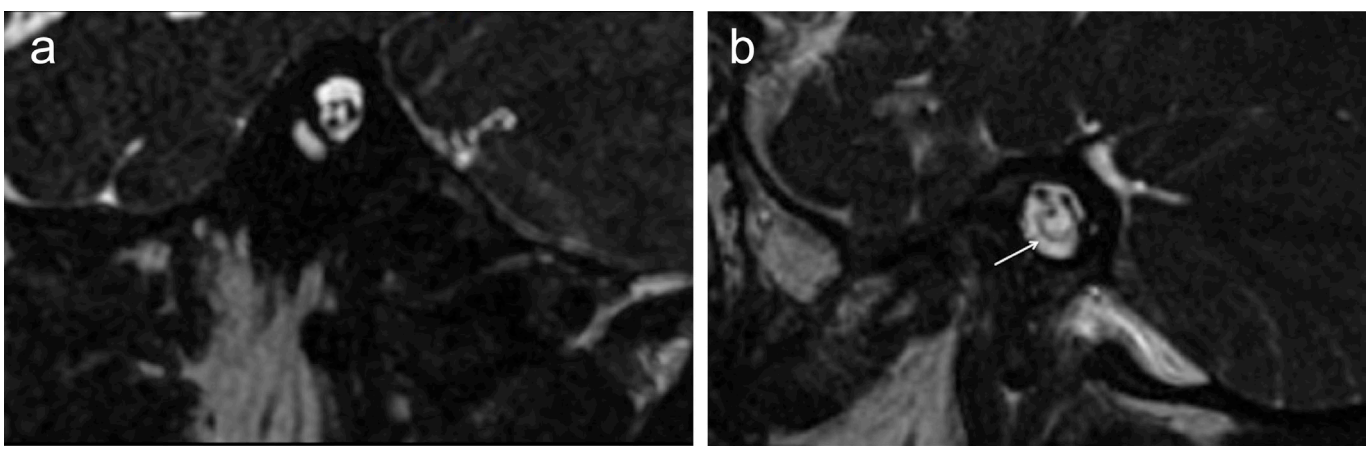

Figure 7. a, b. Normal appearance of vestibulocochlear and facial nerves on sagittal-oblique CISS image from the level of IAC (**a**). The dysmorphic appearance of vestibulocochlear and facial nerves of XLD patient on sagittal-oblique CISS image with curved/comma-shaped appearance of the cochlear nerve (**b**, *arrow*).

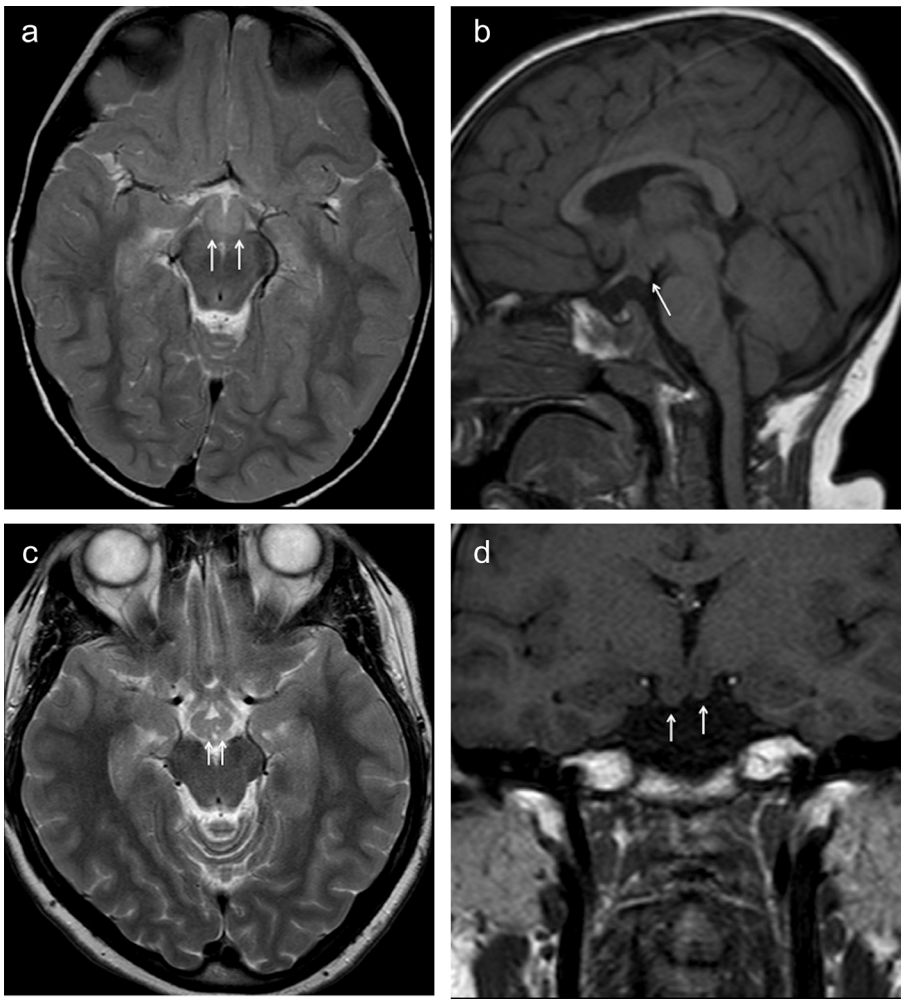

Figure 8. a-d. Axial T2-weighted image (**a**) of a 2-year-old male with XLD reveals thickened hypothalamus (*arrows*). Sagittal T1-weighted image (**b**) shows a 3-year-old male with hypothalamic enlargement (*arrow*). Axial T2-weighted image (**c**) of a 21-year-old female patient shows wrinkly hypothalamus (*arrows*); coronal T1-weighted image (**d**) of the same patient shows asymmetrical hypothalamic hamartoma-like enlargement (*arrows*).

cinereum diverticula in a toddler with XLD. Anderson et al.[3] reported 2 brothers with XLD with identical inner ear findings and hypothalamic malformations which were labeled as hypothalamic hamartomas. Siddiqui et al.[7] reported the varied appearance of hypothalamic malformations ranging from subtle thickening to hamartoma-like enlargement in 12 of 15 patients with XLD and *POU3F4* mutations. Recently, Matifoll et al.[8] reported some features of hypothalamus discriminating from normal controls with high sensitivity and specificity levels in their 10 cases with XLD. These features were the folded appearance of the ventromedial hypothalamus on T2 axial images characterized by an external/internal cleft and a concave morphology of the medial eminence on coronal T2 images. POU genes are related to cell differentiation and organ formation and the *POU3F4* gene encodes a transcription factor, affecting the inner ear, hypothalamus, nervous system, and pituitary gland development, which is the possible mechanism linking the hypothalamic malformations and inner ear deformity.[3] In our study, characteristic dysmorphism of the hypothalamus was seen as thickening to an irregular lobular appearance on axial images in all cases. Among the patients who had MRI, 9 patients (90%) had marked hypothalamic malformations, with asymmetry in 5 (50%) and hamartoma-like appearance in 5 (50%). As XLD patients may have hypothalamic hamartomas, Anderson et al.[3] recommended that the brain MRI in patients with XLD should be assessed accordingly, especially in patients demonstrating inner ear diverticula. However, in our study, the rate of hypothalamic malformations was similar in patients with and without diverticula/cystic structures. It is noteworthy that none of our patients with hypothalamic malformations had any endocrinological symptoms, but laboratory testing had not been performed as they did not have any endocrine dysfunction. Additionally, none of our cases had any history of seizure or epilepsy.

Our study had limitations due to the retrospective design and the limited number of cases. The diagnosis of XLD was based on pathognomonic temporal bone CT findings, and no genetic tests had been performed. Additionally, the relatively smaller number of patients with MRI was also a limiting factor.

In conclusion, XLD has pathognomonic inner ear imaging findings including IP-III with accompanying hypothalamic malformations including hypothalamic thickening and associated hamartoma-like appearance. In this anomaly, the cochlea appears to be dysplastic, with decreased transverse and slightly increased vertical dimensions, and this is an important finding as it could affect the selection of the cochlear implant type.

Conflict of interest disclosure

The authors declared no conflicts of interest.

References

1. Talbot JM, Wilson DF. Computed tomographic diagnosis of X-linked congenital mixed deafness, fixation of the stapedial footplate, and perilymphatic gusher. *Am J Otol*. 1994;15(2):177-182.
2. Phelps PD, Reardon W, Pembrey M, Bellman S, Luxom L. X-linked deafness, stapes gushers and a distinctive defect of the inner ear. *Neuroradiology*. 1991;33(4):326-330. [CrossRef]
3. Anderson EA, Özütemiz C, Miller BS, Moss TJ, Nascene DR. Hypothalamic hamartomas and inner ear diverticula with X-linked stapes gusher syndrome - new associations? *Pediatr Radiol*. 2020;50(1):142-145. [CrossRef]
4. Kumar G, Castillo M, Buchman CA. X-linked stapes gusher: CT findings in one patient. *AJNR Am J Neuroradiol*. 2003;24(6):1130-1132.
5. Sennaroglu L, Bajin MD. Special article: Incomplete partition type III: a rare and difficult cochlear implant surgical indication. *Auris Nasus Larynx*. 2018;45(1):26-32. [CrossRef]
6. Gong WX, Gong RZ, Zhao B. HRCT and MRI findings in X-linked non-syndromic deafness patients with a POU3F4 mutation. *Int J Pediatr Otorhinolaryngol*. 2014;78(10):1756-1762. [CrossRef]
7. Siddiqui A, D'Amico A, Colafati GS, et al. Hypothalamic malformations in patients with X-linked deafness and incomplete partition type 3. *Neuroradiology*. 2019;61(8):949-952. [CrossRef]
8. Prat Matifoll JA, Wilson M, Goetti R, et al. A case series of X-linked Deafness-2 with sensorineural hearing loss, stapes fixation, and perilymphatic gusher: MR imaging and clinical features of

hypothalamic malformations. *AJNR Am J Neuroradiol*. 2020;41(6):1087-1093. [CrossRef]
9. Whitehead MT, Vezina G. Tuber cinereum diverticula in a 28-month-old with Xq21 deletion syndrome. *Case Rep Radiol*. 2014;2014:413574. [CrossRef]
10. Oztunali C, Saylisoy S, Toprak U, Incesulu A. Association between incomplete partition Type III and abnormal hypothalamic morphology: further imaging evidence. *J Comput Assist Tomogr*. 2020;44(5):704-707. [CrossRef]
11. Mori MC, Chang KW. CT analysis demonstrates that cochlear height does not change with age. *AJNR Am J Neuroradiol*. 2012;33(1):119-123. [CrossRef]
12. Sennaroğlu L, Bajin MD. Incomplete partition type III: A rare and difficult cochlear implant surgical indication. *Auris Nasus Larynx*. 2018;45(1):26-32. [CrossRef]
13. Nance WE, Setleff R, McLeod A, et al. X-linked mixed deafness with congenital fixation of the stapedial footplate and perilymphatic gusher. *Birth Defects Orig Artic Ser*. 1971;07(4):64-69.
14. Corvino V, Apisa P, Malesci R, et al. X-linked sensorineural hearing loss: A literature review. *Curr Genomics*. 2018;19(5):327-338. [CrossRef]
15. Sennaroglu L. Histopathology of inner ear malformations: do we have enough evidence to explain pathophysiology? *Cochlear Implants Int*. 2016;17(1):3-20. [CrossRef]
16. Song MH, Choi SY, Wu L, et al. *POU3F4* deficiency causes defects in otic fibrocytes and stria vascularis by different mechanisms. *Biochem Biophys Res Commun*. 2011;404(1):528-533. [CrossRef]
17. Hong R, Du Q, Pan Y. New imaging findings of incomplete partition Type III inner ear malformation and literature review. *AJNR Am J Neuroradiol*. 2020;41(6):1076-1080. [CrossRef]
18. Mei X, Schart-Morén N, Li H, et al. Three-dimensional imaging of the human internal acoustic canal and arachnoid cistern: a synchrotron study with clinical implications. *J Anat*. 2019;234(3):316-326. [CrossRef]
19. Smeds H, Wales J, Asp F, et al. X-linked malformation and cochlear implantation. *Otol Neurotol*. 2017;38(1):38-46. [CrossRef]
20. Alballaa A, Aschendorff A, Arndt S, et al. Incomplete partition type III revisited-long-term results following cochlear implant. *HNO*. 2020;68(Suppl 1):25-32. [CrossRef]
21. Pollak A, Lechowicz U, Kędra A, et al. Novel and de novo mutations extend association of POU3F4 with distinct clinical and radiological phenotype of hearing loss. *PLOS ONE*. 2016;11(12):e0166618. [CrossRef]
22. Bast TH. Development of the otic capsule: I. Resorption of the cartilage in the canal portion of the otic capsule in human fetuses and its relation to the growth of the semicircular canals. *Arch Otolaryngol*. 1932;16(1):19-38. [CrossRef]
23. Ho ML, Moonis G, Halpin CF, Curtin HD. Spectrum of third window abnormalities: semicircular canal dehiscence and beyond. *AJNR Am J Neuroradiol*. 2017;38(1):2-9. [CrossRef]
24. Poretti A, Brehmer U, Scheer I, Bernet V, Boltshauser E. Prenatal and neonatal MR imaging findings in oral-facial-digital syndrome type VI. *AJNR Am J Neuroradiol*. 2008;29(6):1090-1091. [CrossRef]
25. Chung WY, Chung LP. A case of oral-facial-digital syndrome with overlapping manifestations of type V and type VI: a possible new OFD syndrome. *Pediatr Radiol*. 1999;29(4):268-271. [CrossRef]
26. Takanashi J, Tada H, Ozaki H, Barkovich AJ. Malformations of cerebral cortical development in oral-facial-digital syndrome type VI. *AJNR Am J Neuroradiol*. 2009;30(2):E22-E23. [CrossRef]
27. Azukizawa T, Yamamoto M, Narumiya S, Takano T. Oral-facial-digital syndrome type 1 with hypothalamic hamartoma and Dandy-Walker malformation. *Pediatr Neurol*. 2013;48(4):329-332. [CrossRef]
28. Stephan MJ, Brooks KL, Moore DC, Coll EJ, Goho C. Hypothalamic hamartoma in oral-facial-digital syndrome type VI (Varadi syndrome). *Am J Med Genet*. 1994;51(2):131-136. [CrossRef]
29. Squires LA, Constantini S, Miller DC, Wisoff JH. Hypothalamic hamartoma and the Pallister-Hall syndrome. *Pediatr Neurosurg*. 1995;22(6):303-308. [CrossRef]
30. Boudreau EA, Liow K, Frattali CM, et al. Hypothalamic hamartomas and seizures: distinct natural history of isolated and Pallister-Hall syndrome cases. *Epilepsia*. 2005;46(1):42-47. [CrossRef]
31. Diaz LL, Grech KF, Prados MD. Hypothalamic hamartoma associated with Laurence-Moon-Biedl syndrome. Case report and review of the literature. *Pediatr Neurosurg*. 1991-1992;17(1):30-33. [CrossRef]